

# Accuracy of calculations involving $\alpha^3$ vacuum-polarization diagrams: Muonic hydrogen Lamb shift and muon $g-2$

T. Kinoshita\*

*Newman Laboratory of Nuclear Studies, Cornell University, Ithaca, New York 14853*

M. Nio†

*Department of Physics, Nara Women's University, Nara, Japan 630*

(Received 21 December 1998; published 2 August 1999)

The contribution of the  $\alpha^3$  single electron-loop vacuum-polarization diagrams to the Lamb shift of muonic hydrogen has been evaluated recently by two independent methods. One uses the exact parametric representation of the vacuum-polarization function while the other relies on the Padé approximation method. The high precision of these values offers an opportunity to examine the reliability of the Monte Carlo integration as well as that of the Padé method. Our examination covers both the muonic hydrogen atom and muon  $g-2$ . We test them further for the cases involving two-loop vacuum polarization, where an exact analytic result is known. Our analysis justifies the result for the Lamb shift of muonic hydrogen and also resolves the long-standing discrepancy between two previous evaluations of the muon  $g-2$  value. [S0556-2821(99)05215-7]

PACS number(s): 12.20.Ds, 06.20.Jr, 31.30.Jv, 36.10.Dr

## I. INTRODUCTION

In a recent paper we evaluated the contribution  $\Delta E^{(p6)}$  of sixth-order electron-loop vacuum-polarization diagrams to the muonic hydrogen ( $\mu^- p^+$ ) Lamb shift [1]. Together with the proposed measurement of the  $2P_{1/2}-2S_{1/2}$  Lamb shift [2] it will lead to a very precise determination of the proton charge radius.

The most laborious part of this calculation is that of the single electron loop diagrams contributing to the sixth-order vacuum-polarization function (see Fig. 1). Using the parametric representation for this function [3] we find its contribution to the Lamb shift to be [1]

$$\Delta E^{(p6)} = 0.017\ 410\ (9) m_r(Z\alpha)^2 \left(\frac{\alpha}{\pi}\right)^3, \quad (1)$$

where  $m_r$  is the reduced mass of the muon-proton system and  $Z=1$  is the proton charge in units of the electron charge  $|e|$ . As a cross-check, we have also computed  $\Delta E^{(p6)}$  using the Padé approximation of the single electron loop sixth-order vacuum-polarization function  $\Pi_3^{[11]}(z)$ ,  $z = q^2/4m_e^2$ , where  $m_e$  is the electron mass [4]. Inserting the real part of  $\Pi_3^{[11]}$  derived from Eq. (7) of Ref. [4] into Eq. (3) of Ref. [1], we obtained the Lamb shift contribution in the [3/2] and [2/3] Padé approximations. Since they are practically indistinguishable, we will not label them separately and simply quote them as

$$\Delta E_{\text{Re}}^{(p6)} = 0.017\ 414\ 9\ (25) m_r(Z\alpha)^2 \left(\frac{\alpha}{\pi}\right)^3. \quad (2)$$

We also derived the imaginary part of the approximate  $\Pi_3^{[11]}$  and, inserting it in Eq. (6) of Ref. [1], obtained

$$\Delta E_{\text{Im}}^{(p6)} = 0.017\ 414\ 9\ (26) m_r(Z\alpha)^2 \left(\frac{\alpha}{\pi}\right)^3. \quad (3)$$

Again the [3/2] and [2/3] Padé approximations are nearly indistinguishable. The results (2) and (3) are consistent with each other and agree within one standard deviation with the direct calculation (1). Note, however, that the uncertainties in Eqs. (2) and (3) are those caused by numerical treatment of the Padé approximation and do not represent the accuracy of the Padé method itself. To gain insight into how good the Padé approximation is we have examined two cases where exact results are known. Based on these results we argue that the true value of the muonic hydrogen Lamb shift will be found within 0.0007% of the Padé value, which is well within the uncertainties quoted in Eqs. (2) or (3).

## II. DERIVATION OF PADÉ APPROXIMATION RESULTS

Let us begin with a brief review of the derivation of the Padé approximation to the sixth-order vacuum-polarization function  $\Pi_3^{[11]}(z)$ ,  $z = q^2/4m_e^2$ , by Baikov and Broadhurst [4]. The analytic properties of  $\Pi_3^{[11]}(z)$  they utilized are (a) the first three coefficients of the Taylor expansion around  $z=0$ ,

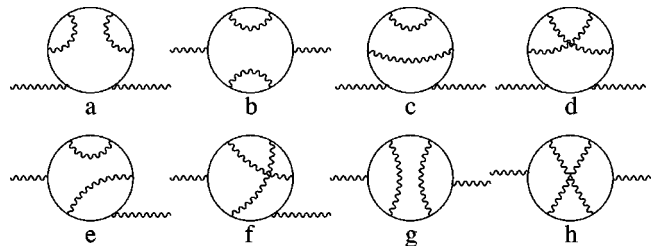


FIG. 1. Sixth-order vacuum-polarization diagrams with a single electron loop.

\*Email address: tk@hepht.cornell.edu

†Email address: makiko@phys.nara-wu.ac.jp

(b) the first two log  $z$ -dependent coefficients of the expansion in  $1/z$  for large negative  $z$ , and (c) the threshold Coulomb behavior which is determined by nonrelativistic quantum mechanics. Taking account of this information they constructed the function

$$\begin{aligned} \tilde{\Pi}_3^{[11]}(z) &\equiv \Pi_3^{[11]}(z) + 4\Pi_2(z) \\ &+ (1-z)G(z) \left( \frac{9}{4}G(z) + \frac{31}{16} + \frac{229}{32z} \right) - \frac{229}{32z} - \frac{173}{96}, \end{aligned} \quad (4)$$

where  $\Pi_2(z)$  is the fourth-order vacuum-polarization function [5].  $G(z)$  is the hypergeometric function  ${}_2F_1(1, 1; \frac{3}{2}; z)$ . For the negative real  $z$ ,  $G$  is given by

$$G(z) = \frac{1}{\sqrt{z^2 - z}} \ln(\sqrt{-z} + \sqrt{1-z}). \quad (5)$$

Analytic continuation of  $G(z)$  from  $z < 0$  to  $z \geq 1$  through the upper  $z$  plane yields

$$\text{Re } G(z) = \frac{-1}{\sqrt{z^2 - z}} \ln(\sqrt{z} + \sqrt{z-1}), \quad (6)$$

$$\text{Im } G(z) = \frac{\pi}{2\sqrt{z^2 - z}}. \quad (7)$$

By construction  $\tilde{\Pi}_3^{[11]}(z)$  is analytic in the  $z$ -plane cut along the real axis  $1 < z < \infty$ . The function defined by

$$\frac{1-\omega}{(1+\omega)^2} [\tilde{\Pi}_3^{[11]} - \tilde{\Pi}_3^{[11]}(-\infty)], \quad z = \frac{4\omega}{(1+\omega)^2}, \quad (8)$$

is analytic for  $|\omega| < 1$ , and may be simulated accurately by a Padé approximant  $P(\omega)$ . Analytic information on  $\tilde{\Pi}_3^{[11]}$  listed above is translated into six data for  $P(\omega)$ :  $\{P(-1), P(0), P'(0), P''(0), P'''(0), P(1)\}$ . Using these data we have constructed

$$P(\omega) = \frac{a_0 + a_1\omega + a_2\omega^2 + a_3\omega^3}{b_0 + b_1\omega + b_2\omega^2 + b_3\omega^3}. \quad (9)$$

The coefficients  $a$ 's and  $b$ 's for both [2/3] and [3/2] Padé approximations calculated from the given data are listed in Table I. Once a Padé approximant is constructed, we can readily obtain the corresponding  $\tilde{\Pi}_3^{[11]}$  from Eqs. (4) and (8).

The  $2P_{1/2} - 2S_{1/2}$  Lamb shift of the muonic hydrogen has been evaluated in two ways. One uses the formula which contains  $\Pi(z)$  for negative  $z$  [1]:

$$\Delta E = \frac{2}{\pi} (Z\alpha)^2 m_r \int_0^\infty da \tilde{\rho}(a^2) \Pi[-a^2/(4\beta^2)], \quad (10)$$

where

TABLE I. Coefficients of Padé approximants. We set  $b_0 = 1$  for the overall normalization.

Coefficient	[2/3] Padé	[3/2] Padé
$a_0$	5.450 103 092	5.450 103 092
$a_1$	-0.966 458 776	-0.891 171 812
$a_2$	-1.785 150 929	-1.800 086 980
$a_3$	0	-0.025 240 917
$b_0$	1	1
$b_1$	-0.456 709 419	-0.442 895 559
$b_2$	-0.121 731 656	-0.128 331 492
$b_3$	0.001 706 927	0

$$\tilde{\rho}(a^2) = \frac{2a^2(1-a^2)}{(1+a^2)^4} \quad (11)$$

and

$$\beta = \frac{m_e}{m_r Z\alpha} = 0.737 \ 383 \ 76 \quad (30). \quad (12)$$

Substituting  $\tilde{\Pi}_3^{[11]}(z)$  determined from Table I in Eq. (10) and evaluating it numerically,<sup>1</sup> we obtained the result (2).

The second approach utilizes the imaginary part of the approximate  $\tilde{\Pi}_3^{[11]}$  for  $z > 1$  obtained from the Padé approximant  $P(\omega)$  by taking its value on the unit circle in the upper-half  $\omega$  plane. Using this information the  $2P_{1/2} - 2S_{1/2}$  Lamb shift of the muonic hydrogen can be expressed by [1]

$$\Delta E = m_r (Z\alpha)^2 \int_1^\infty dz \frac{\text{Im}\Pi(z)}{\pi} \frac{2\beta^2}{(1+2\beta\sqrt{z})^4}. \quad (13)$$

The result (3) follows from Eq. (13).

### III. DISCUSSION

The results (2) and (3) obtained by the Padé approximation method are in good agreement with the direct result (1). The difference between them is within one standard deviation of the result (1) and can be ignored for the purpose of comparison with experiment. However, Eqs. (1), (2), and (3) all involve some uncertainties inherent to their derivation. Thus it will be worthwhile to examine the nature of these uncertainties. There are at least two possible causes which may contribute to these uncertainties: One is that the error estimate generated by VEGAS in the evaluation of Eq. (1) might be a gross underestimate of the true error. The other arises from the fact that the Padé approximant does not represent  $\tilde{\Pi}_3^{[11]}(z)$  accurately for all values of  $z$ .

<sup>1</sup>Unless specified otherwise integrals are evaluated numerically on DEC $\alpha$  using the adaptive-iterative Monte Carlo subroutine VEGAS [6].

### A. Nonstatistical error in VEGAS calculation

The integration routine VEGAS is an adaptive-iterative procedure based on random sampling of the integrand [6]. In the  $i$ th iteration, the integral is evaluated by sampling the integrands at points chosen randomly according to a distribution function chosen in the  $(i-1)$ -st iteration. This generates the approximate value  $I_i$  of the integral, an estimate of its uncertainty  $\sigma_i$ , and the distribution function to be used for the next iteration. After several iterations  $I_i$  and  $\sigma_i$  are combined under the assumption that all iterations are statistically independent. The combined value and error are given by

$$I = \left( \sum_i (I_i / \sigma_i^2) \right) / \left( \sum_i (1 / \sigma_i^2) \right),$$

$$\sigma = \left( \sum_i (1 / \sigma_i^2) \right)^{-1/2}. \quad (14)$$

In general VEGAS is found to converge rapidly for a sufficiently large number of samplings. However, a special care is required when it is applied to the integration of Feynman amplitudes in which renormalization is carried out on the computer relying on point-by-point cancellation of singularities between the unrenormalized integrand and the corresponding renormalization term. This does not pose a problem if we operate with infinite precision. In reality, however, calculation is carried out using finite precision arithmetic, such as double (real\*8) or quadruple (real\*16) precision. Random numbers generated by VEGAS for sampling of the integrand will inevitably hit points very close to some singularity. This will result in evaluation of the difference of two very large and nearly identical numbers with finite amount of significant digits. At such a point most of the significant digits cancel out leaving only a few significant digits or no significant digit at all. (This will be referred to as digit-deficiency or  $d-d$  problem, and the subdomain of integration where this happens, which contains some boundary surface of the hypercube in our problem, will be called the  $d-d$  domain.) This introduces nonstatistical noise in the evaluation of the integral and its error estimate, even though the effect, being confined to the  $d-d$  domain of very small measure, is often not readily distinguishable from the fluctuations inherent to random sampling of the integrand. They tend to give the integral a false value and might cause deviation of error estimate from the assumed statistical behavior. However, the  $d-d$  problem encountered in the  $i$ th iteration will not affect the performance of the  $(i+1)$ -st iteration unless it distorts the distribution function very severely. As is seen from Eq. (14)  $I_i$  with larger  $\sigma_i$  are given smaller weights, giving only small impact on the composite  $I$  and  $\sigma$ . A problem arises, however, if some  $\sigma_i$  is relatively small even if it is suffering from the  $d-d$  problem. In such a case the final  $I$  may be distorted in an unpredictable way.

The relative impact of the  $d-d$  domain decreases as the sampling statistics in an iteration increases. More importantly, it decreases dramatically if quadruple precision is adopted. In the past, however, this was not necessarily a

practical approach because it typically requires 20 or more computing time for execution compared with double precision calculation. Only recently the availability of faster computers has made this a viable option.

Because of higher speed we normally start evaluation of Feynman integrals in double precision. If this runs into a  $d-d$  problem, we split the integration domain into a small region around the  $d-d$  domain and the remainder. The difficult region is then evaluated in quadruple precision, while evaluation of the rest continues in double precision. (In some really difficult cases, it will be preferable to adopt quadruple precision for the entire integration domain.) This strategy has been very successful and many integrals were evaluated very precisely in this manner. In fact, in some cases, the achieved numerical precision was such that it led to uncovering of errors in some analytic or semianalytic calculations [7].

Unfortunately, it is not always easy to detect problems caused by the  $d-d$  distortion. This was the case with some muon  $g-2$  diagrams involving sixth-order vacuum-polarization diagrams [8]. While Ref. [8] reported the value  $-0.2415(19)(\alpha/\pi)^4$  the same diagrams evaluated using the Padé approximation method gave [4]

$$a_\mu^{(8)}(\text{Padé}) = -0.230362 \quad (5) \left( \frac{\alpha}{\pi} \right)^4 \quad (15)$$

which disagreed with Ref. [8] by about 6 standard deviations. The reliability of the error estimate in Ref. [8] was thus called into question.

As was discussed above, the most effective way to separate the  $d-d$  error encountered in double precision from the statistical uncertainty is to go over to quadruple precision. We have therefore repeated the integration of Ref. [8] entirely in quadruple precision with a roughly equal amount of sampling statistics. The new value

$$a_\mu^{(8)}(\text{Fig. 1}) = -0.2285 \quad (18) \left( \frac{\alpha}{\pi} \right)^4 \quad (16)$$

agrees within one standard deviation with the Padé value (15) but disagrees strongly with the old value.

A closer examination of Ref. [8] reveals that some of the eight integrals [in particular, one involving Fig. 1(e), evaluated with 60 million sampling points per iteration] show signs of suffering from the presence of  $d-d$  error. This is now clearly confirmed by the new result (16). One way to overcome this problem within double precision calculation is to go over to much larger statistics. In order to see whether ten times more sampling points per iteration is sufficient for the diagram  $e$ , we have evaluated it in both double<sup>2</sup> and quadruple<sup>3</sup> precisions (with 600 million sampling point per iteration and 60 iterations). The two results are in good agreement showing that the double precision calculation is reliable now. Encouraged by this, we have evaluated the re-

<sup>2</sup>Evaluated on the Fujitsu VX computer at the Computer Center of Nara Women's University.

<sup>3</sup>Evaluated on the IBM SP2 computer at Cornell Theory Center.

maintaining seven integrals in double precision with ten times more statistics. The total contribution is found to be

$$a_\mu^{(8)}(\text{Fig. 1}) = -0.230\ 596\ (416) \left(\frac{\alpha}{\pi}\right)^4. \quad (17)$$

This is in good agreement with the Padé result (15).

We conclude that the problem encountered by the result [8] was caused solely by insufficient statistics. Unfortunately this does not become visible until more extensive calculation is done.

To examine the sensitivity of the Lamb shift calculation to the precision of the arithmetic used we evaluated the sixth-order vacuum-polarization contribution to the muonic hydrogen in both double and quadruple precision. The results obtained in double and quadruple precisions are listed in Table 1 of Ref. [1]. The double precision calculation was carried out using 100 million sampling points per iteration while that of quadruple precision was obtained for 1 million sampling points per iteration [except for diagrams (a) and (e) which employ 2 and 4 times more sampling points, respectively]. As is clearly seen from Table I of Ref. [1], the results in double and quadruple precision are in good agreement and give us confidence that this problem does not suffer visibly from the  $d$ - $d$  problem. The reason why the Lamb shift calculation looks less susceptible to the  $d$ - $d$  problem is that, unlike the muon  $g$ -2 case, the contribution from large momentum transfer region is strongly suppressed by the hydrogenic wave function.

### B. How good is the Padé approximation?

We now want to examine whether or not the Padé result  $a_\mu(\text{Padé})$  of Eq. (15) agrees within its much smaller error bars with the true value of  $a_\mu^{(8)}(\text{Fig. 1})$ . This question is raised because the  $[2/3]$  or  $[3/2]$  Padé approximant  $P(\omega)$  of Eq. (9) does not have complete information on  $\Pi_3^{[1]}$ . In principle it is possible to answer this question by improving the numerical precision of Eq. (17) by two orders of magnitude. This is not very practical, however, since it would require  $10^4$ -fold increase in the computational effort. Another approach is to go to higher-order Padé approximations, taking additional exact properties of  $\Pi_3^{[1]}$  into account [9,10].

Let us instead follow an alternative and easier route, namely, examine how well the Padé method works by applying it to the cases where exact results are known. The first example is the contribution of the two-loop vacuum-polarization to the muon  $g-2$ . The exact result is given by [11]

$$a_\mu^{(6)}(\alpha^2 v.p.) = 1.493\ 671\ 80\ (4) \left(\frac{\alpha}{\pi}\right)^3, \quad (18)$$

where the uncertainty comes only from the uncertainty in the measured value of  $m_\mu/m_e$ . The corresponding value obtained by numerical integration by VEGAS starting from the Källen-Sabry spectral function is

$$a_\mu^{(6)}(\text{K-S}) = 1.493\ 672\ 7\ (40) \left(\frac{\alpha}{\pi}\right)^3. \quad (19)$$

The difference between Eqs. (18) and (19) is well within the error bars of Eq. (19) and will disappear as the numerical precision of Eq. (19) increases.

Meanwhile, the real and imaginary parts of  $[3/2]$  and  $[2/3]$  Padé approximation given in the Appendix produce

$$a_\mu^{(6)}(\text{Padé Re}) = \begin{cases} 1.493\ 677\ 6\ (16) & \cdots [2/3]A, \\ 1.493\ 678\ 1\ (16) & \left(\frac{\alpha}{\pi}\right)^3 \cdots [2/3]B, \\ 1.493\ 676\ 2\ (16) & \cdots [3/2]A, \\ 1.493\ 675\ 9\ (16) & \cdots [3/2]B, \end{cases} \quad (20)$$

and

$$a_\mu^{(6)}(\text{Padé Im}) = \begin{cases} 1.493\ 674\ 2\ (38) & \cdots [2/3]A, \\ 1.493\ 847\ 4\ (38) & \left(\frac{\alpha}{\pi}\right)^3 \cdots [2/3]B, \\ 1.493\ 737\ 9\ (38) & \cdots [3/2]A, \\ 1.493\ 676\ 5\ (38) & \cdots [3/2]B, \end{cases} \quad (21)$$

respectively, where  $A$  and  $B$  refer to two different sets of determinations of Padé functions. Within the context of this approximation it is not possible to tell which of the results (20) and (21) are good or bad. Since the  $[m/n]$  Padé approximation will get closer and closer to the exact function as  $m$  and  $n$  increase, however, the Padé results based on the real and imaginary parts should give identical results in the large  $m$  and  $n$  limit. This means that near equality of results from the real and imaginary parts may be chosen as a working criterion for selecting good Padé approximation. According to this criterion the results  $[2/3]A$  and  $[3/2]B$  are good while  $[2/3]B$  and  $[3/2]A$  are not. Since this is not a rigorous criterion, we may of course choose the worst case as a measure of the uncertainty of the Padé approximation.

The disagreement between better values of Eqs. (20) and (21) and the exact value (18) is about  $0.000006 (\alpha/\pi)^3$  ( $\sim 0.0004\%$ ), which falls somewhat outside the estimated errors of Eqs. (20) and (21). The difference of about  $0.00017 (\alpha/\pi)^3$  ( $\sim 0.01\%$ ) between Eq. (18) and the ‘‘worst’’ value of Eqs. (20) and (21) is much larger, and is well outside its estimated error. Based on these observations we may conclude that the near equality of real and imaginary Padé values is a useful working criterion and indicates that the  $[2/3]$  and  $[3/2]$  Padé methods give results, with a high probability, within  $0.0004\%$  of the exact value. Analogously, the Padé approximation value (15) of an eighth-order muon  $g$ -2 may



not deviate from the true value by more than 0.001%, even allowing for possible differences between  $\Pi_2$  and  $\Pi_3^{[1]}$ , staying within the error bars of Eq. (15).

The second example is the Lamb shift caused by the fourth-order vacuum-polarization function. The Lamb shift evaluated by VEGAS using the exact vacuum-polarization

function [5] is

$$\Delta E_{\text{exact}}^{(p4)} = 0.045\ 922\ 738\ (57)\ m_r(Z\alpha)^2 \left(\frac{\alpha}{\pi}\right)^2, \quad (22)$$

while the real and imaginary parts of the [3/2] and [2/3] Padé approximation described in the Appendix give

$$\Delta E_{\text{Padé Re}}^{(p4)} = \begin{Bmatrix} 0.045\ 923\ 200\ 88 \\ 0.045\ 923\ 320\ 16 \\ 0.045\ 922\ 988\ 50 \\ 0.045\ 922\ 938\ 13 \end{Bmatrix} m_r(Z\alpha)^2 \left(\frac{\alpha}{\pi}\right)^2 \begin{matrix} \dots [2/3]A, \\ \dots [2/3]B, \\ \dots [3/2]A, \\ \dots [3/2]B, \end{matrix} \quad (23)$$

and

$$\Delta E_{\text{Padé Im}}^{(p4)} = \begin{Bmatrix} 0.045\ 923\ 200\ 97 \\ 0.045\ 933\ 403\ 92 \\ 0.045\ 926\ 642\ 63 \\ 0.045\ 922\ 938\ 22 \end{Bmatrix} m_r(Z\alpha)^2 \left(\frac{\alpha}{\pi}\right)^2 \begin{matrix} \dots [2/3]A, \\ \dots [2/3]B, \\ \dots [3/2]A, \\ \dots [3/2]B, \end{matrix} \quad (24)$$

respectively.<sup>4</sup> Uncertainties of all numerical coefficients in Eqs. (23) and (24) do not exceed  $0.5 \times 10^{-9}$ .

The [2/3]A and [3/2]B results of Eqs. (23) and (24) are in good agreement with Eq. (22), the difference being about 0.0007%. Meanwhile the [2/3]B value of Eq. (24) deviates from Eq. (22) by about 0.02%. The six standard deviation difference between Eq. (22) and ‘‘good’’ values of Eqs. (23) and (24) is unlikely to be attributable to the fault of numerical integration. Instead it must be interpreted as the measure of the approximate nature of the [2/3] and [3/2] Padé, which can be remedied only by going to higher-order Padé approximation.

Finally one may ask how can one justify the use of the Padé approximation for the two-loop vacuum-polarization function as a model for the three-loop case, in view of the fact that the three-loop function  $\Pi_3^{[1]}$  has a threshold singularity ( $\sim 1/\nu$ ) while  $\Pi_2$  does not. Our answer is that there is not much analytical difference between  $P(\omega)$  of two-loop and three-loop cases since this singularity is removed explicitly in the construction (8) of the Padé function  $P(\omega)$ .

### C. Conclusion

Based on these considerations we conclude the following. (i) The Lamb shift calculation by numerical integration method gives a reliable result even if double precision arithmetic is used, provided sufficient sampling of the integrand is made in each step of iteration. (ii) The [2/3] and [3/2] Padé methods for the vacuum-polarization function given in Ref.

[4] is a very good approximation over nearly all momentum space region, even though it is exact only at a few chosen values of the momentum. It will be possible to narrow the gap between Padé and exact results by using more input data and by going to higher-order Padé approximations. However, we believe that [2/3] and [3/2] cases are good enough for the purpose of confirming the reliability of numerical integration method.

### ACKNOWLEDGMENTS

We thank K. G. Chetyrkin, J. H. Kühn, R. Harlander, and M. Steinhauser for bringing our attention to Refs. [9,10]. The work of T.K. was supported in part by the U. S. National Science Foundation. The work of M.N. was supported in part by the Grant-in-Aid (No. 10740123) of the Ministry of Education, Science, and Culture, Japan. Part of T.K.’s work was carried out on the SP2 computer at the Cornell Theory Center.

### APPENDIX: PADÉ APPROXIMATION TO $\Pi_2$

The proper two-loop vacuum-polarization function  $\Pi_2$  can be obtained from Eq. (57) of Ref. [5] by removing the contribution of  $(\Pi_1)^2$ , where  $\Pi_1$  is the one-loop vacuum-polarization function. Since  $\Pi_2$  is known explicitly, it can be used to construct a Padé approximant of any degree of precision. Our purpose here is to test the approximation to  $\Pi_3^{[1]}$ . Thus we construct a Padé approximant of  $\Pi_2$  using analytic information similar to those used in constructing  $\Pi_3^{[1]}$  described in Sec. II. They are

- (i) small momentum behavior of  $\Pi_2(z)$  given by [4]

<sup>4</sup>The results (23) and (24) are obtained using the numerical integration routine of MAPLE V.

TABLE II. Coefficients of Padé approximants for two-loop vacuum polarization function  $\Pi_2(z)$ . We set  $b_0=1$  for the overall normalization.

Coefficient	[2/3]A	[2/3]B	[3/2]A	[3/2]B
$a_0$	0.218 599 301	0.218 599 301	0.218 599 301	0.218 599 301
$a_1$	-0.011 600 062	-0.097 946 773	-0.051 634 466	0.005 017 399
$a_2$	-0.118 517 746	-0.176 492 097	-0.190 422 374	-0.143 212 168
$a_3$	0	0	-0.023 342 491	-0.018 586 700
$b_0$	1	1	1	1
$b_1$	-0.228 103 636	-0.623 103 575	-0.411 244 220	-0.152 085 728
$b_2$	-0.470 961 931	-0.667 030 155	-0.767 838 808	-0.597 234 583
$b_3$	0.060 545 956	0.082 509 741	0	0

$$\Pi_2(z) = \frac{82}{81}z + \frac{449}{675}z^2 + \frac{249916}{496125}z^3 + \dots, \quad (\text{A1})$$

(ii) leading terms of  $\Pi_2(z)$  for  $z \rightarrow -\infty$ ,

$$\Pi_2(z) = \frac{5}{24} - \zeta_3 - \frac{1}{4} \ln(-4z) + \frac{1}{z} \left[ -\frac{3}{4} \ln(-4z) \right] + \mathcal{O}\left(\frac{1}{z^2}\right), \quad (\text{A2})$$

(iii) the threshold behavior of the imaginary part of  $\Pi_2(z)$

$$\frac{1}{\pi} \text{Im} \Pi_2(z) = \frac{\pi^2}{4} - 2\delta + \mathcal{O}(\delta^2), \quad (\text{A3})$$

where  $\delta = \sqrt{1-1/z}$ . This means that the real part of  $\Pi_2(z)$  has the logarithmic threshold singularity of the form

$$\Pi_2(z) = -\frac{\pi^2}{4} \ln|1-z| + \dots \quad (\text{A4})$$

To take these analytic properties into account we construct a function  $\tilde{\Pi}_2(z)$  containing five parameters  $c_1, \dots, c_5$ :

$$\tilde{\Pi}_2(z) \equiv \Pi_2(z) + (1-z)G(z)(c_1 + c_2/z) + c_3 + c_4/z + c_5F(z), \quad (\text{A5})$$

where  $G(z)$  is introduced in Eq. (4) and  $F(z) = \ln|1-z|$ . For  $z > 1$ ,  $F(z)$  has the imaginary part

$$\text{Im} F(z) = -\pi. \quad (\text{A6})$$

The coefficients  $c_1$ ,  $c_2$ , and  $c_4$  are determined by requiring cancellation of all logarithmic singularities found in Eqs. (A2) and (A4). The remaining  $c_3$  and  $c_5$  are determined by

requiring that  $\tilde{\Pi}_2$  vanishes in the limit  $z \rightarrow 0_-$ . We find that  $\tilde{\Pi}_2(z)$  is analytic in the  $z$ -plane cut along the real axis ( $1, +\infty$ ) if we choose

$$\begin{aligned} c_1 &= \frac{1}{2}(1 - \pi^2), & c_2 &= \frac{1}{4}(7 - \pi^2), & c_3 &= \frac{1}{12}(1 + 5\pi^2), \\ c_4 &= \frac{1}{4}(-7 + \pi^2), & c_5 &= \frac{1}{4}\pi^2. \end{aligned} \quad (\text{A7})$$

The function to be Padé approximated is chosen as

$$\frac{1}{(1+\omega)^2} [\tilde{\Pi}_2(z) - \tilde{\Pi}_2(-\infty)], \quad z = \frac{4\omega}{(1+\omega)^2}. \quad (\text{A8})$$

We construct the Padé approximant  $P(\omega)$  of the form (9) using Eqs. (A1), (A2), and (A3) as the input data. We obtained two sets of  $a_i$ 's and  $b_i$ 's for each [2/3] and [3/2] Padé approximation, which we denote [2/3]A, [2/3]B, [3/2]A, and [3/2]B. They are listed in Table II. The Padé results of Sec. III B are obtained from this table.

As a final check, we compared directly the imaginary parts of the exact Källén-Sabry function and its Padé approximation. The difference of the two functions  $\Delta \equiv \text{Im} \Pi_2(\text{K-S})/\pi - \text{Im} \Pi_2(\text{Padé})/\pi$  is examined for the entire momentum range  $z \geq 1$ . The fractional deviation  $\Delta/[\text{Im} \Pi_2(\text{K-S})/\pi]$  is less than 0.2% in all cases of the Padé approximations. The Padé approximation functions are found to oscillate around the exact value. Also, by integrating  $\Delta$  over the entire range of  $\delta = \sqrt{1-1/z}$ ,  $0 \leq \delta \leq 1$ , we found

$$\int_0^1 d\delta \Delta = \begin{cases} 0.000 276 & \dots [2/3]A, \\ -0.000 930 & \dots [2/3]B, \\ -0.000 461 & \dots [3/2]A, \\ 0.000 015 & \dots [3/2]B. \end{cases} \quad (\text{A9})$$

Apparently the values of the muon  $g-2$  and Lamb shift are more accurate than are implied by these results.

- [1] T. Kinoshita and M. Nio, Phys. Rev. Lett. **82**, 3240 (1999).
- [2] D. Taqqu *et al.*, Hyperfine Interact. **101/102**, 599 (1996).
- [3] T. Kinoshita and W. B. Lindquist, Phys. Rev. D **27**, 853 (1983).
- [4] P. A. Baikov and D. J. Broadhurst, in *New Computing Techniques in Physics Research IV*, edited by B. Denby and D. Perret-Gallix (World Scientific, Singapore, 1995), pp. 167–172.
- [5] G. Källén and A. Sabry, K. Dan. Vidensk. Selsk. Mat. Fys. Medd. **29**, 1 (1955).
- [6] G. P. Lepage, J. Comput. Phys. **27**, 192 (1978).
- [7] T. Kinoshita, Phys. Rev. Lett. **75**, 4728 (1995); T. Kinoshita and M. Nio, Phys. Rev. D **53**, 4909 (1996).
- [8] T. Kinoshita, Phys. Rev. D **47**, 5013 (1993).
- [9] K. G. Chetyrkin, R. Harlander, J. H. Kühn, and M. Steinhauser, Nucl. Phys. **B503**, 339 (1997).
- [10] K. G. Chetyrkin, J. H. Kühn, and M. Steinhauser, Nucl. Phys. **B505**, 40 (1997).
- [11] S. Laporta, Nuovo Cimento A **106**, 675 (1993).